

# iREVIEWS

STATE OF-THE-ART PAPER

## Magnetic Resonance Spectroscopy in Myocardial Disease

Lucy E. Hudsmith, MA, MRCP, Stefan Neubauer, MD, FRCP  
*Oxford, United Kingdom*

Magnetic resonance spectroscopy (MRS) is the only noninvasive, nonradiation exposure technique for the investigation of cardiac metabolism *in vivo*. MRS uses magnetic resonance signals from nuclei, such as  $^{31}\text{P}$  phosphorus,  $^1\text{H}$  hydrogen, and  $^{23}\text{Na}$  sodium, to provide comprehensive metabolic and biochemical information about cardiac muscle. This method is highly versatile and can provide metabolic insights into the role of cardiac metabolism, in particular, cardiac energetics, in a wide number of conditions, including hypertensive, valvular, and ischemic heart disease, heart failure, and cardiac transplantation, as well as cardiomyopathies. This method can also be used to monitor patient responses to therapeutic interventions: pharmacologic, surgical, or interventional. When combined with cardiovascular magnetic resonance imaging, MRS enables detailed pathophysiologic insights into the inter-relations among cardiac structure, function, perfusion, and metabolism. However, MRS is currently used primarily as a research tool because of low temporal and spatial resolution and low reproducibility. It is hoped that future technical developments and use of higher magnetic field strengths (such as 7-T) may enable application of cardiac MRS in clinical practice. (J Am Coll Cardiol Img 2009;2:87–96) © 2009 by the American College of Cardiology Foundation

Cardiovascular magnetic resonance (CMR) is a widespread imaging technique, used extensively in clinical cardiology, which uses the nuclear spin of protons in fat and water to provide detailed anatomical and functional images. Magnetic resonance spectroscopy (MRS) is the only noninvasive imaging modality that provides insight into metabolic components of cardiac muscle *in vivo* without the use of an external tracer. MRS not only detects signal from protons, but also from other nuclei with a nuclear spin including  $^{23}\text{Na}$  sodium (Na),  $^{13}\text{C}$  carbon (C), and  $^{31}\text{P}$  phosphorus (P).  $^1\text{H}$ -MRS allows detection of a number of metabolites, including total creatine, lactate, deoxyhemoglobin, and fatty ac-

ids;  $^{31}\text{P}$ -MRS enables detection of adenosine triphosphate (ATP) and phosphocreatine;  $^{13}\text{C}$  assesses the metabolic pathways of glycolysis, the tricarboxylic acid cycle or beta-oxidation; and  $^{23}\text{Na}$ -magnetic resonance imaging (strictly speaking, not a spectroscopy method, but listed here because it provides biochemical information) allows detection of myocardial tissue sodium content (1,2).

However, these nonproton nuclei have a significantly lower magnetic resonance sensitivity than  $^1\text{H}$  hydrogen ( $^1\text{H}$ ) and are present in concentrations 4 to 5 orders of magnitude lower than those of  $^1\text{H}$  nuclei of water and fat. As a result, the temporal and spatial resolution of MRS severely limits its current clinical

application. Presently, MRS is technically difficult, requires lengthy scans, and specialist expertise, as well as additional magnetic resonance hardware and software. However, with improvement in data acquisition and analysis techniques, many theoretical and clinical questions may be addressed and answered by cardiac MRS.

The aim of this review is to provide an overview of the principles of cardiac MRS and recent MRS advances, and to discuss clinical research applications of MRS in myocardial disease, particularly ischemic heart disease and heart failure.

### Human Cardiac MRS

The majority of human cardiac MRS studies have investigated the  $^{31}\text{P}$  nucleus. The first  $^{31}\text{P}$ -magnetic resonance spectra from human myocardium were obtained in the 1980s (3).

Cardiac MRS uses the same hardware as CMR, for patients, typically a 1.5- or 3.0-T magnet (ultra-field [7- to 18-T] for experimental studies), with additional hardware including nucleus-specific coils (e.g.,  $^{31}\text{P}$ -coil) and a broadband radiofrequency transmitter to excite nonproton nuclei. Specific MRS acquisition sequences, MRS post-processing, and data analysis packages are also required.

Subjects are studied in the prone position to minimize the distance between the surface coil and the heart and to minimize respiratory motion. The magnetic resonance spectrometer consists of a superconducting magnet interfaced with a computer and a radiofrequency transmitter and receiver (Fig. 1). Before acquisition, the

magnetic field must first be homogenized with shim gradients.

With the patient in the prone position,  $^1\text{H}$  CMR are first acquired to allow appropriate anatomical voxel selection for spectroscopic interrogation (Fig. 2). One of several localization sequences, such as depth-resolved surface coil spectroscopy (DRESS), image-selected in vivo spectroscopy (ISIS), or 3-dimensional chemical shift imaging (3D-CSI), which enables selection of multiple voxels in 3 dimensions, is required to obtain signal from a voxel positioned within the myocardium excluding  $^{31}\text{P}$  signal from overlapping skeletal muscle (4,5).

A radiofrequency pulse leads to spin excitation and the resulting magnetic resonance signal, the

free induction decay (FID), is converted into a magnetic resonance spectrum, which relates resonance frequency to signal intensity, by Fourier transformation. A number of signal-averaged acquisitions yield a magnetic resonance spectrum with sufficient signal-to-noise ratio. Correction factors for saturation and blood contamination are applied, and the area under each resonance is then proportional to the amount of each  $^{31}\text{P}$  nucleus species in the heart, allowing direct quantification of the relative concentrations of each metabolite (2). Absolute quantification of metabolite concentrations, although preferable, is more complex, requiring calibration of the  $^{31}\text{P}$  signal to the  $^1\text{H}$  water signal of the voxel (6). Another technique, spectral localization with optimum pointspread function (SLOOP), enables interrogation of curved voxels, shaped to the heart, and absolute quantification using a  $^{31}\text{P}$  reference standard, flip angle calibration, B1 field mapping, and determination of myocardial mass within the interrogated voxel (7).

A typical  $^{31}\text{P}$  spectrum from a healthy subject shows 6 resonances: 3  $^{31}\text{P}$  atoms (alpha, beta, and gamma) of ATP, phosphocreatine (PCr), 2,3-diphosphoglycerate (from erythrocytes), and phosphodiester (from membrane and serum phospholipids) (Fig. 2).

Cardiac  $^{31}\text{P}$ -MRS, by means of the PCr-to-ATP ratio, provides an index of the energetic state of the heart. The creatine kinase (CK) energy shuttle ensures thermodynamic control of the cell, maintaining a low concentration of free adenosine diphosphate near the mitochondria, and providing ATP to the myofibrils for muscle contraction. When demand for ATP outweighs ATP synthesis (such as in ischemia), PCr levels fall, resulting in a low PCr-to-ATP ratio; ATP levels fall only when PCr levels are substantially depleted, because the CK equilibrium constant strongly favors ATP synthesis above PCr synthesis (8). A second mechanism decreasing the PCr-to-ATP ratio is a reduction in the total creatine pool, as it occurs in heart failure.

At 1.5-T, required  $^{31}\text{P}$ -MRS voxels are 20 to 70 ml, the acquisition time 20 to 40 min, yielding a variability of 15% for PCr-to-ATP ratios (9). These factors are the major limitation of clinical cardiac MRS, and future developments and technical advances of MRS will have to deliver substantial improvements to make the method valuable for clinical practice.

#### ABBREVIATIONS AND ACRONYMS

**ATP** = adenosine triphosphate

**CK** = creatine kinase

**CMR** = cardiovascular magnetic resonance imaging

**HCM** = hypertrophic cardiomyopathy

**MRS** = magnetic resonance spectroscopy

**NYHA** = New York Heart Association

**$^{31}\text{P}$ -MRS** =  $^{31}$ phosphorus-magnetic resonance spectroscopy

**PCr/ATP** = phosphocreatine-to-adenosine triphosphate

**3D-CSI** = 3-dimensional chemical shift imaging

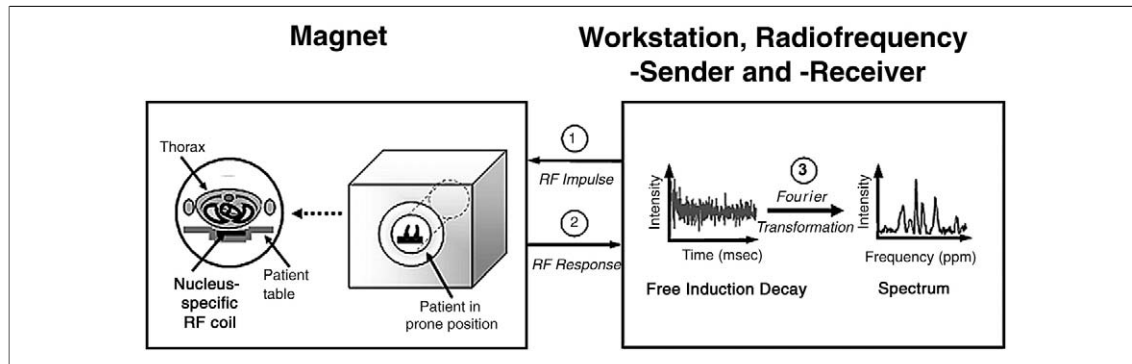


**Figure 1. Schematic Illustration of a Human Cardiac Magnetic Resonance Spectroscopy Study**

The radiofrequency (RF) generator and workstation create an RF impulse, which is sent to the nucleus-specific RF coil to excite the nuclear spins in the heart. The coil detects the RF response, which is relayed to the computer and stored as the free induction decay. Fourier transformation results in a magnetic resonance spectrum. Reprinted, with permission, from Hudsmith and Neubauer (65).

### Other Nuclei

Protons ( $^1\text{H}$ ) have the highest MR sensitivity, so  $^1\text{H}$ -MRS theoretically has the greatest potential for clinical application.  $^1\text{H}$  is present in a large number of metabolites, including creatine, lactate, carnitine, taurine, and the  $-\text{CH}_3$  and  $-\text{CH}_2$  resonances of lipids. Measurement of total creatine, combined with  $^{31}\text{P}$ -MRS, allows noninvasive quantification of adenosine diphosphate and free energy change of ATP hydrolysis (10), and tissue deoxygenation can be quantified using oxymyoglobin and deoxymyoglobin resonances (11). Current technical limitations for  $^1\text{H}$ -MRS include the need to suppress the strong water signal and the need for identification of overlapping resonances.

At present, there are no clinical cardiac studies using  $^{13}\text{C}$ -MRS because of its low sensitivity and

the requirement of exogenous  $^{13}\text{C}$ -labelled precursors to detect a signal. However, in principle, quantification of cardiac substrate use, the citric acid cycle, and pyruvate dehydrogenase flux or beta-oxidation of fatty acids may be possible, as has been shown in experimental models (12,13).

$^{23}\text{Na}$ -magnetic resonance imaging can be used to investigate and identify myocardial infarction and viability (14). The total  $^{23}\text{Na}$  signal is elevated in scar and correlates with histologically identified infarct scar (see the following text).

### Clinical CMR Spectroscopy Studies

The main clinical areas in which cardiac MRS may provide insight into pathophysiologic mechanisms are ischemic heart disease, heart failure, transplantation, and cardiomyopathies.

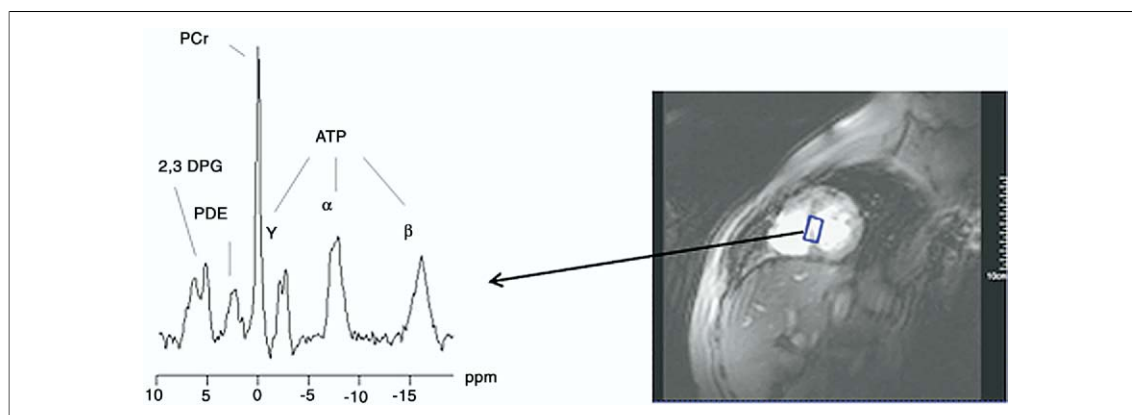


**Figure 2.  $^{31}\text{P}$  Magnetic Resonance Spectroscopy in a Healthy Volunteer**

$^{31}\text{P}$  magnetic resonance spectrum using 3D chemical shift imaging in a healthy volunteer. The 6 resonances correspond to the 3  $^{31}\text{P}$  atoms of adenosine triphosphate (ATP) (alpha, beta, and gamma), phosphocreatine (PCr), 2,3-diphosphoglycerate (2,3-DPG), and phosphodiester (PDE).  $^1\text{H}$  short-axis image showing localization of the voxel in the myocardial interventricular septum. Reprinted, with permission, from Hudsmith and Neubauer (65).

Using  $^{31}\text{P}$ -MRS, the cardiac PCr-to-ATP ratios of healthy subjects range between 1.1 and 2.5, with some evidence for a decrease in high-energy phosphates with increasing age (4,15,16). This large variation reflects methodologic variation of acquisition and analysis techniques, emphasizing the need for development and standardization of these techniques.

In normal volunteers as well as in athletes' hearts (rowers and cyclists), PCr-to-ATP ratios remain constant except under extreme pharmacologic stimulation, when there is a modest reduction (17). In contrast, hypertensive patients with pathological hypertrophy have reduced PCr-to-ATP ratios at rest and during pharmacologic stimulation, with these values correlating inversely with parameters of diastolic function (18).  $^{31}\text{P}$ -MRS therefore provides insight into cardiac energy metabolism differences in pathological and physiological hypertrophy and may, in the future, provide a method to differentiate these when screening athletes before competitive selection.

### Ischemic Heart Disease

Identification of the metabolic changes in normally perfused, ischemic, or scarred myocardium, combining stress testing with  $^{31}\text{P}$ -MRS is a potentially powerful tool to assess exercise-induced regional ischemia without the need for contrast agents or radiation. Within seconds of reduced oxygenation, PCr levels fall and inorganic phosphate levels increase (19). The feasibility of detecting this clinically has been shown by Weiss et al (20), who demonstrated that in patients with  $\geq 70\%$  stenosis of the left anterior descending coronary artery, PCr-to-ATP ratios were normal at rest, significantly decreased from  $1.5 \pm 0.3$  to  $0.9 \pm 0.2$ , with a 30% to 35% increase in cardiac work with hand-grip exercise, and then returned to  $1.27 \pm 0.38$  after recovery. After revascularization, PCr-to-ATP ratios remained stable during the repeated exercise.

Buchthal et al. (21) and Johnson et al. (22) showed that myocardial PCr-to-ATP ratios decreased by  $25 \pm 15\%$  with hand grip exercise in females with chest pain and normal luminal coronary arteries, and at 3-year follow-up, an initially abnormal  $^{31}\text{P}$ -MRS stress test was a strong predictor of future cardiovascular events. These findings suggest microvascular dysfunction and tissue ischemia as mechanisms for chest pain in this patient cohort.

Thus,  $^{31}\text{P}$ -MRS stress testing might prove to be a valuable technique for investigating myocardial

ischemia, monitoring response to interventional or medical therapies, and being a prognostic tool. However, ischemic heart disease is spatially heterogeneous, requiring high spatial resolution of signal acquisition, and the low resolution and high measurement variability of MRS currently limits its value for regional assessment of ischemia in individual patients.

Cardiac  $^{31}\text{P}$  spectroscopy can identify viable (stunned or hibernating myocardium in which ATP levels remain near normal [23]); in nonviable necrotic and scarred territories,  $^{31}\text{P}$ -MRS demonstrated complete absence of PCr (24,25). However, nonviable scar tissue results in a reduction in both PCr and ATP, so the ratio cannot assess the degree of loss of viable tissue. Measurement of absolute concentrations of high-energy phosphates has shown that absolute myocardial ATP content was significantly reduced in patients with fixed thallium defects, i.e., nonviable scar tissue, but remained constant in those with viable myocardium (26). Although potentially valuable as a nonstress, non-contrast method for assessing myocardial viability, again,  $^{31}\text{P}$ -MRS is currently limited by its low spatial resolution.

Bottomley and Weiss (27) investigated and validated the use of water suppressed  $^1\text{H}$ -MRS to measure total myocardial creatine content in 10 patients with a history of myocardial infarction and in an animal model of infarction after ligation of the left anterior descending coronary artery. They demonstrated that creatine concentrations were significantly lower in the infarcted myocardium of patients compared with their noninfarcted myocardium, and with healthy controls, and this was confirmed by biopsy studies in the animal model.  $^1\text{H}$ -MRS has a higher sensitivity than  $^{31}\text{P}$ -MRS, so it has a more realistic potential than  $^{31}\text{P}$ -MRS to become a clinical tool to noninvasively identify viable myocardium with intrinsic contrast.

Myocardial total  $^{23}\text{Na}$  signal is increased in both acute necrosis and chronic myocardial scar, but not in viable myocardium (28), so  $^{23}\text{Na}$ -magnetic resonance may provide another approach to investigating myocardial viability based on intrinsic contrast (Table 1). For example, in acute myocardial infarction patients, areas of increased  $^{23}\text{Na}$  signal intensity have been shown to correlate with regional wall motion abnormalities (29), and follow-up studies have demonstrated that the scar  $^{23}\text{Na}$  content remains significantly increased in the long term (30). Although  $^{23}\text{Na}$ -magnetic resonance is a potentially exciting noninvasive method of assessing

myocardial viability, significant technical developments are needed to improve its spatial resolution.

One of the great strengths of MRS is that, in principle, ischemic, scarred (nonviable), and hibernating myocardium can be identified by a combination of <sup>31</sup>P-, <sup>23</sup>Na-, and <sup>1</sup>H-MRS measurements (Table 1). Thus, if the technical hurdles can be overcome, they would provide an attractive set of tools to fully characterize myocardial tissue states in coronary artery disease.

### Heart Failure and Transplantation

Altered cardiac energy metabolism is a characteristic feature of heart failure (31). Clinical <sup>31</sup>P-MRS studies have shown that PCr-to-ATP ratios decrease in advanced heart failure, but initially remain normal. These decreased PCr-to-ATP ratios in patients with dilated cardiomyopathy correlate with the New York Heart Association (NYHA) functional class (32) and left ventricular ejection fraction (33), and they are a marker for prognosis: the PCr-to-ATP ratio was a better predictor of long-term survival than NYHA functional class or left ventricular ejection fraction (34).

However, in heart failure, both PCr and ATP decrease in parallel, so PCr-to-ATP ratios cannot detect the full extent of these changes. Using absolute quantification with the spectral localization with optimum pointspread function (SLOOP) technique, dilated cardiomyopathy patients showed a 51% reduction in absolute PCr levels, a 35% reduction in absolute ATP, and a 25% decrease in PCr-to-ATP ratio (35). Therefore, PCr-to-ATP ratios underestimate the true extent of metabolic derangement in heart failure.

The most sensitive indicators of deranged cardiac energetics in heart failure may be ATP turnover rates. Weiss et al. (36) directly measured ATP flux through the creatine kinase (CK) reaction in normal and failing human hearts using image-guided 4-angle saturation transfer (FAST) <sup>31</sup>P-MRS quantification of CK flux. There was an 18% reduction in cardiac PCr concentration in the heart failure patients compared with healthy controls, with no reduction in ATP levels. In contrast, ATP turnover rates via CK were substantially reduced, by 50%, compared with those in healthy controls. This group has also shown that CK flux is reduced by 30% in hypertrophied hearts with maintained left ventricular function (37). These data illustrate that measures of ATP turnover rates are the most

**Table 1. Characterization of Ischemic, Scarred, or Stunned Myocardium Using <sup>31</sup>P, <sup>1</sup>H, and <sup>23</sup>Na Magnetic Resonance Spectroscopy**

MRS Metabolite	Ischemia	Scar (Nonviable)	Stunned
ATP ( <sup>31</sup> P-MRS)	↓	↓↓	↔
PCr ( <sup>31</sup> P-MRS)	↓	↓↓	↔ or ↓
pHi ( <sup>31</sup> P-MRS)	↓	↔	↔ or ↓
Na ( <sup>23</sup> Na-MRS)	↑	↑	↔
Total creatine ( <sup>1</sup> H-MRS)	↔	↓↓	↔
Deoxyoglobin ( <sup>1</sup> H-MRS)	↑	↔	↔

Reprinted, with permission, from Neubauer (64).  
 ATP = adenosine triphosphate; MRS = magnetic resonance spectroscopy.

sensitive indicators of energetic derangement in the heart.

<sup>1</sup>H-MRS has also demonstrated significant reductions in total creatine levels in dilated cardiomyopathy patients, which correlated with left ventricular ejection fraction (38). Pharmacologic treatment of heart failure with energy-sparing medications such as beta-blockers, angiotensin-converting enzyme inhibitors, and angiotensin II receptor blockers improves outcome. In a small number of dilated cardiomyopathy patients who were treated with beta-blockers, angiotensin-converting enzyme inhibitors, diuretics, and digoxin for 3 months, PCr-to-ATP ratios improved from 1.51 ± 0.32 to 2.15 ± 0.27 within 3 months in association with clinical improvement (Fig. 3) (32).

In a recent randomized, double-blind, cross-over study, 12 heart failure patients, on conventional therapy, were randomized to trimetazidine, a metabolic modulator partially inhibiting fatty acid oxidation and stimulating glucose use, or placebo. Patients underwent physiological testing, echocardiography, and <sup>31</sup>P-MRS (39). Trimetazidine improved NYHA functional class and left ventricular function. Trimetazidine also resulted in a 33% significant increase in PCr-to-ATP ratios, from 1.35 ± 0.33 to 1.80 ± 0.50. Thus, trimetazidine appears to improve cardiac energetics in heart failure. This study also demonstrated that <sup>31</sup>P-MRS can be used to monitor the energetic response to heart failure treatment. However, this is a small study with only 12 patients, and clearly, further large randomized trials of trimetazidine and other metabolic modulators are required to reach definitive conclusions.

Another interesting recent study showed that patients with dilated cardiomyopathy can undergo a long-term exercise program without any detrimental effects on cardiac energetics (40). Furthermore, it is conceivable that the use of absolute changes in

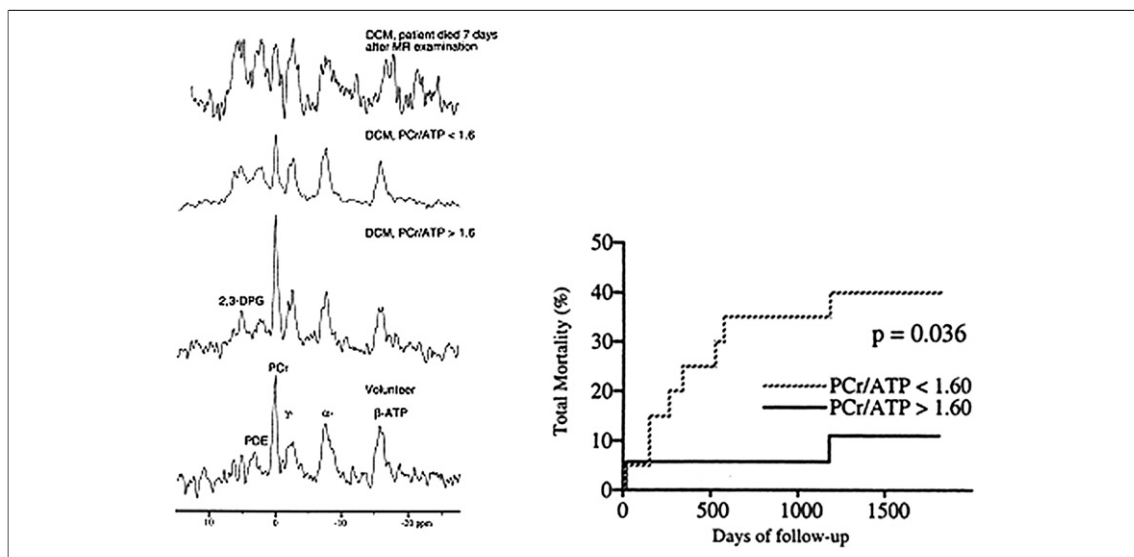


**Figure 3.**  $^{31}\text{P}$  Magnetic Resonance Spectroscopy in Heart Failure Patients

(Left)  $^{31}\text{P}$ -MRS (from top) volunteer, dilated cardiomyopathy (DCM) with normal PCr-to-ATP ratio, DCM with reduced PCr-to-ATP ratio, DCM with severely reduced PCr-to-ATP ratio. (Right) Kaplan-Meier life table analysis for total mortality of patients with dilated cardiomyopathy. Patients were divided into two groups according to PCr-to-ATP ratios (<1.60 and >1.60). Patients with a reduced PCr-to-ATP ratio had an increased mortality over the study period compared with those with a higher ratio ( $p = 0.036$ ). Reprinted, with permission, from Neubauer et al. (34). Abbreviations as in Figure 2.

PCr and ATP and of ATP turnover rates, as surrogate markers for prognosis, in combination with functional assessment using CMR, will aid drug trials in heart failure patients in the future.

Early identification of cardiac transplant rejection is of paramount clinical importance to optimize and target appropriate medical therapy. Using  $^{31}\text{P}$ -MRS, PCr-to-ATP ratios have been shown to be reduced in both animal models (41) and patients with histologic signs of rejection, although no correlation was seen with biopsy scores (42). Exercise  $^{31}\text{P}$ -MRS was investigated by Evanochko et al. (43), who showed a decrease in PCr-to-ATP ratios during exercise in some patients, although again, histologic scores of rejection have not correlated with cardiac energetics. Further work is needed to clarify whether these techniques can be applied to predict transplant rejection in patients (43).

### Valvular Heart Disease

Patients with symptomatic heart failure from valvular heart disease (both aortic stenosis and mitral regurgitation) have been shown to have reduced PCr-to-ATP ratios in comparison with clinically asymptomatic patients. PCr-to-ATP ratios correlated with left ventricular end-diastolic pressures and with end-diastolic wall stress in aortic stenosis and left ventricular end-diastolic and end-systolic

diameter as well as left ventricular wall thickness and left atrial dimensions in mitral regurgitation (44–46). In a group of patients after aortic valve surgery for aortic stenosis,  $^{31}\text{P}$ -MRS has been used to follow the recovery of PCr-to-ATP ratios; these improved significantly from  $1.28 \pm 0.17$  to  $1.47 \pm 0.14$  9 months post-operatively (47). However, a long-term prospective study using cardiac MRS is needed to identify whether  $^{31}\text{P}$ -MRS can provide information about the optimal timing of surgical valve replacement.

### Inherited Cardiomyopathies

$^{31}\text{P}$ -MRS has the potential to noninvasively phenotype cardiomyopathies due to specific gene defects such as hypertrophic cardiomyopathy (HCM). HCM is associated with myocardial energy depletion secondary to inefficient force generation (48).  $^{31}\text{P}$ -MRS has demonstrated reduced PCr-to-ATP ratios in these patients, with a more pronounced energetic derangement in patients with a family history of HCM (49,50). Impaired PCr-to-ATP ratios have been demonstrated even in young asymptomatic patients, illustrating that the energetic derangement occurs early in the disease process (51).

Furthermore, future studies might enable  $^{31}\text{P}$ -MRS to phenotype different HCM genotypes from

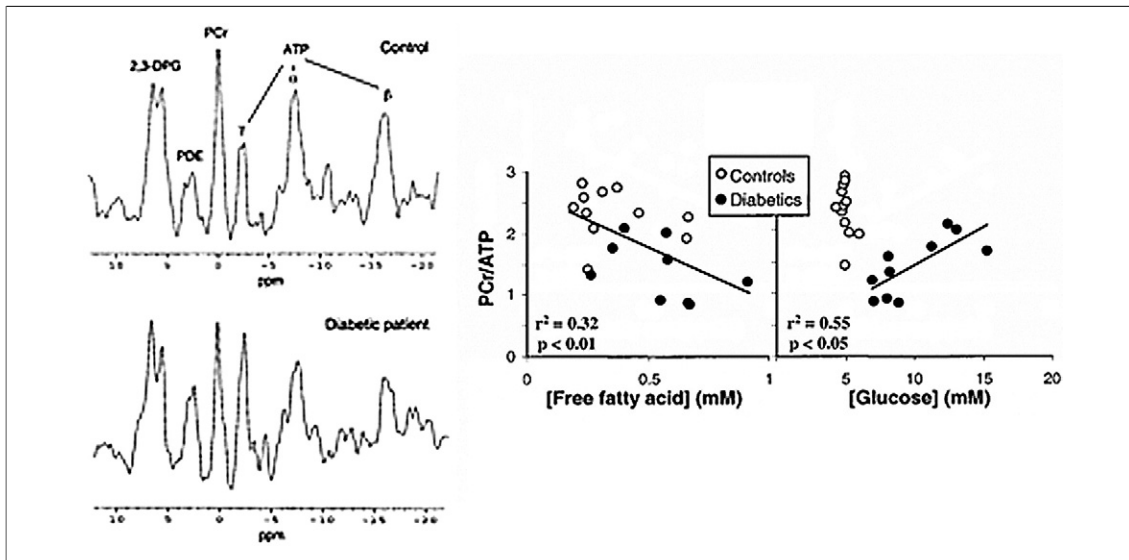


**Figure 4. Impaired Cardiac Energy Metabolism in Patients With Type 2 Diabetes**

(Left)  $^{31}\text{P}$  MR spectra in a healthy control subject (top) and a patient with type 2 diabetes mellitus (bottom) showing reduced PCr-to-ATP ratio in the patient. (Right) Correlation of energetic derangement with fatty acid and glucose metabolism. PCr-to-ATP ratios correlated negatively with plasma free fatty acid concentrations for all subjects ( $r^2 = 0.32$ ,  $p = 0.01$ ) and positively with plasma glucose concentration ( $r^2 = 0.55$ ,  $p = 0.05$ ) for the diabetic patients. Abbreviations as in Figure 2. Reprinted, with permission, from Scheuermann-Freestone et al. (55).

PCr-to-ATP ratios at rest or in response to physiologic and pharmacologic stress. The metabolic responses of patients, in combination with the detailed anatomical, functional, and scar imaging provided by CMR, may identify prognostic indicators that could aid in risk stratification and family screening of relatives of HCM patients.

Patients and female carriers of Becker muscular dystrophy with preserved left ventricular function have reduced PCr-to-ATP ratios in comparison with healthy volunteers (52). These findings may provide insight into the metabolic mechanisms of contractile failure and the development of cardiomyopathy as well as identify targets and tools for monitoring potential therapeutic intervention. Altered cardiac energetics have also been identified in patients with hereditary hemochromatosis (53) and familial hypercholesterolemia, in whom values normalized after statin therapy (54).

### Diabetes, Obesity, and Diets

$^{31}\text{P}$ -MRS studies of patients with diabetes (both types 1 and 2) and normal left ventricular ejection fraction have shown reduced PCr-to-ATP ratios, which correlate with increased plasma levels of free fatty acids and markers of diastolic function (Fig. 4) (55,56). These findings suggest a potential mecha-

nism for the later development of cardiomyopathy in this patient population.

A recent study by McGavock et al. (57) combined  $^1\text{H}$  MRS and MR imaging in patients with type 2 diabetes mellitus, obesity, impaired glucose tolerance, and in lean normoglycemic individuals, to investigate the relationship between cardiac steatosis and the development of cardiomyopathy. Cardiac steatosis, detected by  $^1\text{H}$ -MRS was iden-

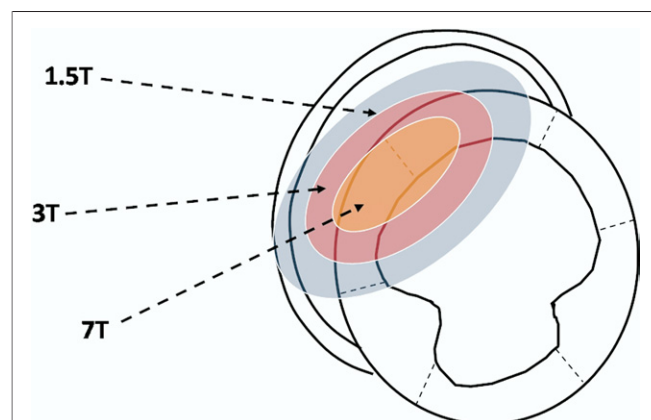


**Figure 5. Improved Resolution of MRS Voxel Sizes With Increasing Field Strength: 1.5-T, 3-T, and 7-T**

A schematic short-axis of the left ventricle and voxel position and sizes at 1.5-, 3-, and 7-T. Figure is courtesy of Dr. Matthew Robson, OCMR, Oxford, United Kingdom. MRS = magnetic resonance spectroscopy.

tified in patients with impaired glucose tolerance, even before the development of type 2 diabetes mellitus. Early identification of such patients at risk may enable therapeutic interventions to normalize myocardial triglyceride metabolism and prevent the development of diabetes and potential subsequent cardiomyopathy.

Using a combination of  $^1\text{H}$ -MRS,  $^{31}\text{P}$ -MRS, and MR imaging, van der Meer et al. showed that a short-term, very low-calorie diet in healthy male subjects resulted in increased myocardial triglyceride levels and impaired diastolic function, with no change in myocardial PCr-to-ATP ratios (58). These data illustrate that the metabolic effects of diet on the heart can be detected. MRS may provide insights into the early cardiac metabolic changes in diabetes and obesity that may lead to cardiomyopathy and help identify potential therapeutic targets to prevent pathological left ventricular remodeling.

### Future Direction

The future of cardiac spectroscopy and its application to clinical cardiology is reliant on a number of technical improvements. The greatest technical improvements are expected from increased magnetic field strengths ( $>3\text{-T}$ ), which result in a linear increase in signal to noise (59) and therefore allow improvements in spatial resolution, temporal resolution, or both. Figure 5 shows an analysis of improvements in voxel sizes when field strength is increased from 1.5- to 3- to 7-T, indicating that at 7-T, we may finally be able to achieve proper coverage of the entire heart with a spatial resolution corresponding to the American Heart Association 17-segment model ( $\sim 8\text{ ml}$ )—something currently not feasible at 1.5- or 3-T.

At these higher field strengths, it should also be possible to achieve substantially higher temporal resolution, which will enable dynamic regional changes in metabolites to be investigated, e.g.,

during stress protocols in patients with ischemic heart disease. In this way, biochemical ergometry may finally become a clinical reality.

Additional advances in coil design (e.g., phased array [60]) and sequence development (61) should also make significant contributions to improving resolution and reproducibility of human cardiac MRS.

Potentially the most advanced recent developments in MRS are efforts to massively increase the MRS signal by dynamic nuclear polarization (or hyperpolarization), which can boost the signal by a factor of up to 100,000. At this point, the method is entirely experimental where it has been shown to quantify metabolic reactions such as Krebs cycle flux (62) and other metabolic pathways. Imaging of intracellular pH is another exciting new experimental capability (63). Regulatory approval of hyperpolarized agents for use in humans and the short half-life of the enhanced signal (minutes) are major hurdles to be overcome.

### Conclusions

MRS provides fundamental insights into cardiac metabolism, and in particular, energetics, in cardiac disease states as well as in response to therapeutic intervention, without the need for external tracers or exposure to radiation (64,65). Although this technique is currently not yet used outside of the research setting, with further technical developments leading to improved temporal and spatial resolution, cardiac MRS has the ability to dramatically advance our understanding of the pathophysiology and metabolic nature of a number of cardiac conditions, especially in patients with heart failure, ischemic heart disease, and inherited cardiomyopathies.

**Reprint requests and correspondence:** Dr. Stefan Neubauer, John Radcliffe Hospital, University of Oxford, Cardiovascular Medicine, Headley Way, Oxford, Oxfordshire OX3 9DU, United Kingdom. *E-mail:* stefan.neubauer@cardiov.ox.ac.uk.

### REFERENCES

1. Ingwall JS. Phosphorus nuclear magnetic resonance spectroscopy of cardiac and skeletal muscles. *Am J Physiol* 1982;242:H729-44.
2. Neubauer S. *Cardiac Magnetic Resonance Spectroscopy. Established and Emerging Applications*: London, United Kingdom, Taylor and Francis Group LLC, 2003.
3. Bottomley PA. Noninvasive study of high-energy phosphate metabolism in human heart by depth-resolved  $^{31}\text{P}$  NMR spectroscopy. *Science* 1985; 229:769-72.
4. Bottomley PA. MR spectroscopy of the human heart: the status and the challenges. *Radiology* 1994;191: 593-612.
5. Pohmann R, von Kienlin M. Accurate phosphorus metabolite images of the human heart by 3D acquisition-weighted CSI. *Magn Reson Med* 2001;45:817-26.
6. Bottomley PA, Atalar E, Weiss RG. Human cardiac high-energy phosphate metabolite concentrations by 1D-resolved NMR spectroscopy. *Magn Reson Med* 1996;35: 664-70.
7. Meininger M, Landschutz W, Beer M, et al. Concentrations of human cardiac phosphorus metabolites determined by SLOOP  $^{31}\text{P}$  NMR spectroscopy. *Magn Reson Med* 1999;41: 657-63.

8. Bessman SP, Geiger PJ. Transport of energy in muscle: the phosphoryl-creatine shuttle. *Science* 1981;211:448-52.
9. Lamb HJ, Doornbos J, den Hollander JA, et al. Reproducibility of human cardiac <sup>31</sup>P-NMR spectroscopy. *NMR Biomed* 1996;9:217-27.
10. Bottomley PA, Weiss RG. Noninvasive localized MR quantification of creatine kinase metabolites in normal and infarcted canine myocardium. *Radiology* 2001;219:411-8.
11. Kreutzer U, Mekhamer Y, Chung Y, Jue T. Oxygen supply and oxidative phosphorylation limitation in rat myocardium in situ. *Am J Physiol Heart Circ Physiol* 2001;280:H2030-7.
12. Lewandowski ED, Doumen C, White LT, LaNoue KF, Damico LA, Yu X. Multiplet structure of <sup>13</sup>C NMR signal from glutamate and direct detection of tricarboxylic acid (TCA) cycle intermediates. *Magn Reson Med* 1996;35:149-54.
13. Malloy CR, Jones JG, Jeffrey FM, Jessen ME, Sherry AD. Contribution of various substrates to total citric acid cycle flux and anaplerosis as determined by <sup>13</sup>C isotopomer analysis and O<sub>2</sub> consumption in the heart. *Magma* 1996;4:35-46.
14. Horn M, Weidensteiner C, Scheffer H, Przyklenk K, von Kienlin M, Neubauer S. Use of <sup>23</sup>Na MRS to discriminate viable from non viable tissue: experimental studies. *Magma* 2000;11:42-3.
15. Kostler H, Landschutz W, Koeppel S, et al. Age and gender dependence of human cardiac phosphorus metabolites determined by SLOOP <sup>31</sup>P MR spectroscopy. *Magn Reson Med* 2006;56:907-11.
16. Okada M, Mitsunami K, Inubushi T, Kinoshita M. Influence of aging or left ventricular hypertrophy on the human heart: contents of phosphorus metabolites measured by <sup>31</sup>P MRS. *Magn Reson Med* 1998;39:772-82.
17. Pluim BM, Lamb HJ, Kayser HW, et al. Functional and metabolic evaluation of the athlete's heart by magnetic resonance imaging and dobutamine stress magnetic resonance spectroscopy. *Circulation* 1998;97:666-72.
18. Lamb HJ, Beyerbacht HP, van der Laarse A, et al. Diastolic dysfunction in hypertensive heart disease is associated with altered myocardial metabolism. *Circulation* 1999;99:2261-7.
19. Clarke K, O'Connor AJ, Willis RJ. Temporal relation between energy metabolism and myocardial function during ischemia and reperfusion. *Am J Physiol* 1987;253:H412-21.
20. Weiss RG, Bottomley PA, Hardy CJ, Gerstenblith G. Regional myocardial metabolism of high-energy phosphates during isometric exercise in patients with coronary artery disease. *N Engl J Med* 1990;323:1593-600.
21. Buchthal SD, den Hollander JA, Merz CN, et al. Abnormal myocardial phosphorus-31 nuclear magnetic resonance spectroscopy in women with chest pain but normal coronary angiograms. *N Engl J Med* 2000;342:829-35.
22. Johnson BD, Shaw LJ, Buchthal SD, et al. Prognosis in women with myocardial ischemia in the absence of obstructive coronary disease: results from the National Institutes of Health-National Heart, Lung, and Blood Institute-Sponsored Women's Ischemia Syndrome Evaluation (WISE). *Circulation* 2004;109:2993-9.
23. Flameng W, Vanhaecke J, Van Belle H, Borgers M, De Beer L, Minten J. Relation between coronary artery stenosis and myocardial purine metabolism, histology and regional function in humans. *J Am Coll Cardiol* 1987;9:1235-42.
24. von Kienlin M, Rosch C, Le Fur Y, et al. Three-dimensional <sup>31</sup>P magnetic resonance spectroscopic imaging of regional high-energy phosphate metabolism in injured rat heart. *Magn Reson Med* 1998;39:731-41.
25. Friedrich J, Apstein CS, Ingwall JS. <sup>31</sup>P nuclear magnetic resonance spectroscopic imaging of regions of remodeled myocardium in the infarcted rat heart. *Circulation* 1995;92:3527-38.
26. Yabe T, Mitsunami K, Inubushi T, Kinoshita M. Quantitative measurements of cardiac phosphorus metabolites in coronary artery disease by <sup>31</sup>P magnetic resonance spectroscopy. *Circulation* 1995;92:15-23.
27. Bottomley PA, Weiss RG. Non-invasive magnetic-resonance detection of creatine depletion in non-viable infarcted myocardium. *Lancet* 1998;351:714-8.
28. Horn M, Weidensteiner C, Scheffer H, et al. Detection of myocardial viability based on measurement of sodium content: a (<sup>23</sup>Na)-NMR study. *Magn Reson Med* 2001;45:756-64.
29. Sandstede JJ, Pabst T, Beer M, et al. Assessment of myocardial infarction in humans with (<sup>23</sup>Na) MR imaging: comparison with cine MR imaging and delayed contrast enhancement. *Radiology* 2001;221:222-8.
30. Sandstede JJ, Hillenbrand H, Beer M, et al. Time course of <sup>23</sup>Na signal intensity after myocardial infarction in humans. *Magn Reson Med* 2004;52:545-51.
31. Neubauer S. The failing heart—an engine out of fuel. *N Engl J Med* 2007;356:1140-51.
32. Neubauer S, Krahe T, Schindler R, et al. <sup>31</sup>P magnetic resonance spectroscopy in dilated cardiomyopathy and coronary artery disease. Altered cardiac high-energy phosphate metabolism in heart failure. *Circulation* 1992;86:1810-8.
33. Neubauer S, Horn M, Pabst T, et al. Contributions of <sup>31</sup>P-magnetic resonance spectroscopy to the understanding of dilated heart muscle disease. *Eur Heart J* 1995;16 Suppl O:115-8.
34. Neubauer S, Horn M, Cramer M, et al. Myocardial phosphocreatine-to-ATP ratio is a predictor of mortality in patients with dilated cardiomyopathy. *Circulation* 1997;96:2190-6.
35. Beer M, Seyfarth T, Sandstede J, et al. Absolute concentrations of high-energy phosphate metabolites in normal, hypertrophied, and failing human myocardium measured noninvasively with (<sup>31</sup>P)-SLOOP magnetic resonance spectroscopy. *J Am Coll Cardiol* 2002;40:1267-74.
36. Weiss RG, Gerstenblith G, Bottomley PA. ATP flux through creatine kinase in the normal, stressed, and failing human heart. *Proc Natl Acad Sci U S A* 2005;102:808-13.
37. Smith CS, Bottomley PA, Schulman SP, Gerstenblith G, Weiss RG. Altered creatine kinase adenosine triphosphate kinetics in failing hypertrophied human myocardium. *Circulation* 2006;114:1151-8.
38. Nakae IMK, Omura T, Yabe T, et al. Proton magnetic resonance spectroscopy can detect creatine depletion associated with the progression of heart failure in cardiomyopathy. *J Am Coll Cardiol* 2003;42:1587-93.
39. Fragasso G, Perseghin G, De Cobelli F, et al. Effects of metabolic modulation by trimetazidine on left ventricular function and phosphocreatine/adenosine triphosphate ratio in patients with heart failure. *Eur Heart J* 2006;27:942-8.
40. Beer M, Wagner D, Myers J, et al. Effects of exercise training on myocardial energy metabolism and ventricular function assessed by quantitative phosphorus-31 magnetic resonance spectroscopy and magnetic resonance imaging in dilated cardiomyopathy. *J Am Coll Cardiol* 2008;51:1883-91.
41. Fraser CD Jr., Chacko VP, Jacobus WE, et al. Early phosphorus <sup>31</sup> nuclear magnetic resonance bioenergetic changes potentially predict rejection in heterotopic cardiac allografts. *J Heart Transplant* 1990;9:197-204.

42. Bottomley PA, Weiss RG, Hardy CJ, Baumgartner WA. Myocardial high-energy phosphate metabolism and allograft rejection in patients with heart transplants. *Radiology* 1991;181:67-75.
43. Evarocho WT, Buchthal SD, den Hollander JA, et al. Cardiac transplant patients response to the (31)P MRS stress test. *J Heart Lung Transplant* 2002;21:522-9.
44. Conway MA, Allis J, Ouwerkerk R, Niioka T, Rajagopalan B, Radda GK. Detection of low phosphocreatine to ATP ratio in failing hypertrophied human myocardium by <sup>31</sup>P magnetic resonance spectroscopy. *Lancet* 1991;338:973-6.
45. Conway MA, Bottomley PA, Ouwerkerk R, Radda GK, Rajagopalan B. Mitral regurgitation: impaired systolic function, eccentric hypertrophy, and increased severity are linked to lower phosphocreatine/ATP ratios in humans. *Circulation* 1998;97:1716-23.
46. Neubauer S, Horn M, Pabst T, et al. Cardiac high-energy phosphate metabolism in patients with aortic valve disease assessed by <sup>31</sup>P-magnetic resonance spectroscopy. *J Investig Med* 1997;45:453-62.
47. Beyersbacht HP, Lamb HJ, van Der Laarse A, et al. Aortic valve replacement in patients with aortic valve stenosis improves myocardial metabolism and diastolic function. *Radiology* 2001;219:637-43.
48. Ashrafian H, Redwood C, Blair E, Watkins H. Hypertrophic cardiomyopathy: a paradigm for myocardial energy depletion. *Trends Genet* 2003;19:263-8.
49. Crilley JG, Boehm EA, Blair E, et al. Hypertrophic cardiomyopathy due to sarcomeric gene mutations is characterized by impaired energy metabolism irrespective of the degree of hypertrophy. *J Am Coll Cardiol* 2003;41:1776-82.
50. Jung WI, Hoess T, Bunse M, et al. Differences in cardiac energetics between patients with familial and non-familial hypertrophic cardiomyopathy. *Circulation* 2000;101:E121.
51. Jung WI, Sieverding L, Breuer J, et al. <sup>31</sup>P NMR spectroscopy detects metabolic abnormalities in asymptomatic patients with hypertrophic cardiomyopathy. *Circulation* 1998;97:2536-42.
52. Crilley JG, Boehm EA, Rajagopalan B, et al. Magnetic resonance spectroscopy evidence of abnormal cardiac energetics in Xp21 muscular dystrophy. *J Am Coll Cardiol* 2000;36:1953-8.
53. Schocke MF, Zoller H, Vogel W, et al. Cardiac phosphorus-31 two-dimensional chemical shift imaging in patients with hereditary hemochromatosis. *Magn Reson Imaging* 2004;22:515-21.
54. Schocke MF, Martinek M, Kremser C, et al. 3-hydroxy-3-methylglutaryl coenzyme A reductase inhibitors improve myocardial high-energy phosphate metabolism in men. *J Cardiovasc Magn Reson* 2003;5:595-602.
55. Scheuermann-Freestone M, Madsen PL, Manners D, et al. Abnormal cardiac and skeletal muscle energy metabolism in patients with type 2 diabetes. *Circulation* 2003;107:3040-6.
56. Metzler B, Schocke MF, Steinboeck P, et al. Decreased high-energy phosphate ratios in the myocardium of men with diabetes mellitus type I. *J Cardiovasc Magn Reson* 2002;4:493-502.
57. McGavock JM, Lingvay I, Zib I, et al. Cardiac steatosis in diabetes mellitus: a <sup>1</sup>H-magnetic resonance spectroscopy study. *Circulation* 2007;116:1170-5.
58. van der Meer RW, Hammer S, Smit JW, et al. Short-term caloric restriction induces accumulation of myocardial triglycerides and decreases left ventricular diastolic function in healthy subjects. *Diabetes* 2007;56:2849-53.
59. Tyler DJ, Hudsmith LE, Clarke K, Neubauer S, Robson MD. A comparison of cardiac (31)P MRS at 1.5 and 3 T. *NMR Biomed* 2008;21:793-8.
60. Lee RF, Giaquinto R, Constantinides C, Souza S, Weiss RG, Bottomley PA. A broadband phased-array system for direct phosphorus and sodium metabolic MRI on a clinical scanner. *Magn Reson Med* 2000;43:269-77.
61. Speck O, Scheffler K, Hennig J. Fast <sup>31</sup>P chemical shift imaging using SSFP methods. *Magn Reson Med* 2002;48:633-9.
62. Merritt ME, Harrison C, Storey C, Jeffrey FM, Sherry AD, Malloy CR. Hyperpolarized <sup>13</sup>C allows a direct measure of flux through a single enzyme-catalyzed step by NMR. *Proc Natl Acad Sci U S A* 2007;104:19773-7.
63. Gallagher FA, Kettunen MI, Day SE, et al. Magnetic resonance imaging of pH in vivo using hyperpolarized <sup>13</sup>C-labelled bicarbonate. *Nature* 2008;453:940-3.
64. Neubauer S. Cardiac MR spectroscopy. In: Manning W, editor. *Atlas of Cardiovascular Magnetic Resonance Imaging*. Philadelphia, PA: Current Medicine Group, 2008.
65. Hudsmith LE, Neubauer S. Detection of myocardial disorders by magnetic resonance spectroscopy. *Nat Clin Pract Cardiovasc Med* 2008;5 Suppl 2:S49-56.

---

**Key Words:** magnetic resonance spectroscopy ■ high-energy phosphates ■ adenosine triphosphate ■ phosphocreatine ■ noninvasive metabolic imaging ■ <sup>31</sup>P spectroscopy ■ cardiac energetics.